Journal of Applied Mathematics and Physics, 2023, 11, 2913-2922
https://www.scirp.org/journal/jamp
ISSN Online: 2327-4379
ISSN Print: 2327-4352

The Kinematics Performance of Self-Propelled Full Freedom Filament in Wakes of Flow around Cylinder

Jiyao Yang, Yun Liu, Guoyi He

The School of Aircraft Engineering, Nanchang Hangkong University, Nanchang, China
Email: jiyaoyang1019@163.com

How to cite this paper: Yang, J.Y., Liu, Y. and He, G.Y. (2023) The Kinematics Performance of Self-Propelled Full Freedom Filament in Wakes of Flow around Cylinder. *Journal of Applied Mathematics and Physics*, **11**, 2913-2922.
https://doi.org/10.4236/jamp.2023.1110192

Received: September 26, 2023
Accepted: October 20, 2023
Published: October 23, 2023

Abstract

In vortex streets, the kinematics performance of self-propelled full freedom filament is closely related to the length and the position of filaments in the flow field. In this paper, the changes of passive propulsion velocity and pressure of full-degree-of-freedom filaments after cylindrical wake were analyzed by 15 sets of experiments when the length and position of filaments were changed. The results show that the propulsive velocity of the filament, it approximately increases first and then decreases with the filament length increasing, and the further away from the center of the cylinder, the smaller the propulsive velocity of the filament. In addition, the longer the filament length and the further it is from the center of the cylinder, the lower the pressure around the filament. Experiments show that filaments without energy input can obtain energy from the surrounding flow field to maintain self-propelled motion. Studying the influence of length and position on the kinematics of filaments is helpful to provide a reference for revealing the hydrodynamic mechanism on passive propulsion process and developing low resistance energy harvesting device in swimming fish movement.

Keywords

Length Position Change, Full Freedom Filaments, Passive Propulsion

1. Introduction

Passive propulsion of swimming fish is a classic fluid mechanics topic, which has promoted the interest of many researchers because of its complex energy conversion and fluid mechanics mechanism for a long time. Researchers found that the passive fish movement in the flow field is affected by many factors, such as the flow field structure, position of fish in the flow field, etc., that is, under certain circumstances, fish can reduce the energy consumption to maintain movement, even perform propulsive motions while being completely passive.

In recent years, many researchers have concentrated on passive propulsion movement of swimming fish [1] [2] [3]. Rosis [4] found the individual hydrodynamic action in fish school is nonlinear, and its propulsion velocity is related to its location. Becker [5] used the passive propulsive flapping wing model to study the hydrodynamic mechanism, the results showed that there are promoting and inhibiting effects between two strings of passive propulsive flapping wings, which led to the existence of two coupling modes of fast and slow propulsive velocity, so that both flapping wings could save energy, they also found that the hydrodynamic effect between individuals plays an important role in the spontaneous maintenance of regular formation of fish. Wang Liang [6] used the passive propulsion hydrofoil model to study the propulsion characteristics of inverted triangle fish school and found that there is a "narrow channel effect" energy saving mechanism, that is, the rear fish would use the trailing vortex of the front two fish to increase velocity and save energy, but the front two fish would increase energy consumption. Hemelrijk [7] studied the propulsive characteristics of fish in different formations, individual fish could achieve higher propulsive efficiency in school than alone except for dense and parallel formations, this is the reason because the downstream fish obtained energy from the upstream tail vortex. Zhu [8] used two tandem flexible filaments to simulate passive propulsion of fish swimming, showed the downstream filament always maintained the same forward velocity and fixed distance with the upstream filament after a period of movement, and always passed through the vortex core of the upstream filament wakes, and its energy consumption is less than that of the upstream filament or a single filament, this phenomenon is that the downstream filament head absorbed energy from the tail vortex generated by the upstream filament. Previous studies have shown that swimming fish can obtain energy from surrounding fluids.

The preliminary passively propelled flexible filaments simulation model [9] generally adopted the degrees of freedom that horizontal [10] or vertical is fixed of filaments to simulate the fish movement [11], and the filament movement is restricted in a certain direction, but real fish movement cannot be well simulated in the research process, the influence of size and position changes cannot be fully explored. In this paper, we will apply a full degree of freedom passive propulsion flexible filament model, extend the problem of constraining a certain direction. The purpose of this paper is to investigate the influence of the length and position of the full freedom flexible filaments on the performance of passive propulsion by the immersed boundary method [12], and to summarize the law of the flow field pressure and propulsion velocity changed with the length and position. The research results are intended to provide theoretical reference for revealing the activity rules of fish, developing low resistance energy harvesting device in swimming fish movement and exploring the hydrodynamics mechanism in the swimming process.

2. Physical Model and Numerically Method

2.1. Physical Model

In this paper, the numerical simulation is carried out by the immersed boundary method. The experimental device is shown in Figure 1. The left side is a rigid cylinder and the right side is a flexible filament, both of which are placed in a two-dimensional uniform incompressible flow from left to right. The cylinder is fixed and diameter is l ($l = 1$), free filament is located directly behind the cylinder and can move freely in the x and y directions, U_∞ represents incoming flow velocity; D represents the horizontal distance between the head of the filament and the center of the cylinder; L is filament length. In the experiment, the influence of the change of length position on the kinematics performance of the filament is analyzed by changing the variables D and L. The calculation regions in this article are: $-5l < x < 20l$ and $-8l < y < 8l$. The middle encryption area is $-l < x < 6l$ and $-2l < y < 2l$, and the grid spacing is $\Delta h/l = 0.02$.

2.2. Numerically Method

The governing equation is:

$$\frac{\partial u}{\partial t} = \nabla \cdot (uu) = -\nabla p + \frac{1}{Re}\nabla^2 u + f \tag{1}$$

$$\nabla \cdot u = 0 \tag{2}$$

$$f(x,t) = \int_0^{L_b} F(X(s),t)\,\delta(x - X(s))\,\mathrm{d}s \tag{3}$$

$$U(X(s),t) = \int_\Omega u(x,t)\,\delta(x - X(s))\,\mathrm{d}x \tag{4}$$

In the above formula, $u(x,t)$ is the fluid velocity, $p(x,t)$ is the fluid pressure, Re is the dimensionless Reynolds number, $Re = \rho d U_\infty / \mu$, F is the introduced external force, representing the force on the fluid caused by the immersed object boundary, X is the coordinate of the filament, the force between the immersed boundary and the flow field is calculated by the immersion boundary method, and the update of the filament position is as follows:

$$\frac{\partial X}{\partial t} = U(X(s),t) \tag{5}$$

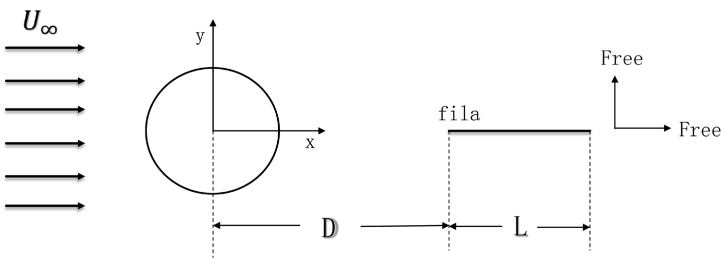

Figure 1. Schematic contour of calculation model.

where, $X(s)$ is the position coordinate of the filament, and s represents the Lagrangian coordinate of the filament, whose boundary conditions are defined as follows: Free boundary condition of the filament head ($s = 0$): $X(s=0,t=0)=(x_0,0)$, $\partial^2 X/\partial s^2=(0,0)^{\mathrm{T}}$, free boundary condition of the tail of the filament ($s = L$): $T = 0$, $\partial^2 X/\partial s^2=(0,0)^{\mathrm{T}}$.

The interaction between the immersion boundary and the fluid consists of two components:

$$F(s,t)=F_1(s,t)+F_2(s,t) \tag{6}$$

$F(s,t)$ is the interaction force between the fluid and the immersed boundary, where $F_1(s,t)$ is the interaction force between the fluid and the solid cylinder, and $F_2(s,t)$ is the interaction force between the fluid and the flexible filament. The equation $F_2(s,t)$ for the interaction between the fluid and the flexible filament is calculated as follows:

$$F_2(s,t)=F_s(s,t)+F_b(s,t)=\frac{\partial T\hat{\boldsymbol{\tau}}}{\partial s}+\frac{\partial E_b}{\partial X} \tag{7}$$

$$T=K_s\left(\left|\frac{\partial \boldsymbol{X}}{\partial s}\right|-1\right) \tag{8}$$

$$\hat{\boldsymbol{\tau}}=\frac{\dfrac{\partial \boldsymbol{X}}{\partial s}}{\left|\dfrac{\partial \boldsymbol{X}}{\partial s}\right|} \tag{9}$$

$$E_b=\frac{1}{2}K_b\int\left|\frac{\partial^2 \boldsymbol{X}(s,t)}{\partial s^2}\right|^2\mathrm{d}s \tag{10}$$

$F_s(s,t)$ is the tensile force and compression force of the filament; $F_b(s,t)$ is the bending force; T is the tension of the filament, which is obtained from Hooke's law. For details, see Formula (8). $\hat{\boldsymbol{\tau}}$ is defined on the filaments each point unit tangent vector, as shown in formula (9). E_b is the bending energy of the filament, see Equation (10). K_s is the tensile coefficient of the filament ($K_s = 1 \times 10^2$). K_b is the bending stiffness of the filament.

In Lin's study [13], by simulating the oscillation of a cylinder in a uniform flow and the motion of filaments in a cylindrical turbulent flow, the solution program used in this paper is verified to be correct.

3. Calculation Results and Analysis

Both the cylinder and the filament are placed in a two-dimensional uniform incompressible flow from left to right, and the experiments are completed under the condition of the Reynolds number of the flow $Re = 150$. The changes in the motion state of the filament are observed by changing the length of the filament L and the distance D between the filament and the center of the cylinder.

3.1. Kinematic Analysis of Filament Propulsion

Under the above conditions, the distance D from the tip of the filament to the center of the cylinder and the length L of the filament are changed. A total of 15 sets of experiments are conducted (see Table 1).

In Table 1, "√" indicates that the filament can complete the passive propulsive motion under this condition, and "×" means that it cannot. The results show that the conditions required for the filaments to complete the passive propulsion motion in the cylindrical wake are strict, and only 7 out of 15 experiments can be completed.

The filaments that can complete self-propelled motion all have a common feature: the filaments have a forward speed in the flow field. This can be well illustrated in the vorticity contour of the velocity streamline. (Figure 2) The selected working condition is $D = 1.0$; $L = 0.5/0.75/1.0/1.25$. Analyze the velocity flow line between the two vortex bands, and the arrow indicates the velocity direction. There is a forward velocity distributed around the filaments, so the filaments can move forward.

The experimental results of seven groups of self-propelled motion show that the velocity of filament propulsion is different in every working condition in the process of passive propulsion. In Table 2, the three values corresponding to each working condition are respectively the average velocity of 0 - 0.5 s, 0.5 - 1.0 s and 1.0 - 1.5 s after the release of the filament. Under the same working condition, the propulsion velocity of the filament gradually increases with time. The propulsion velocity in each working condition from 0 to 0.5 s is the minimum value under the working condition. The velocity increases at 0.5 - 1.0 s and further increases at 1.0 - 1.5 s.

Table 3 shows the average propulsive velocity of the filaments within 1.5 s

Table 1. Experimental results of filaments.

$Re = 150$	$L = 0.5$	$L = 0.75$	$L = 1.0$	$L = 1.25$	$L = 1.5$
$D = 1.0$	√	√	√	√	×
$D = 1.5$	×	√	√	×	×
$D = 2.0$	×	×	√	×	×

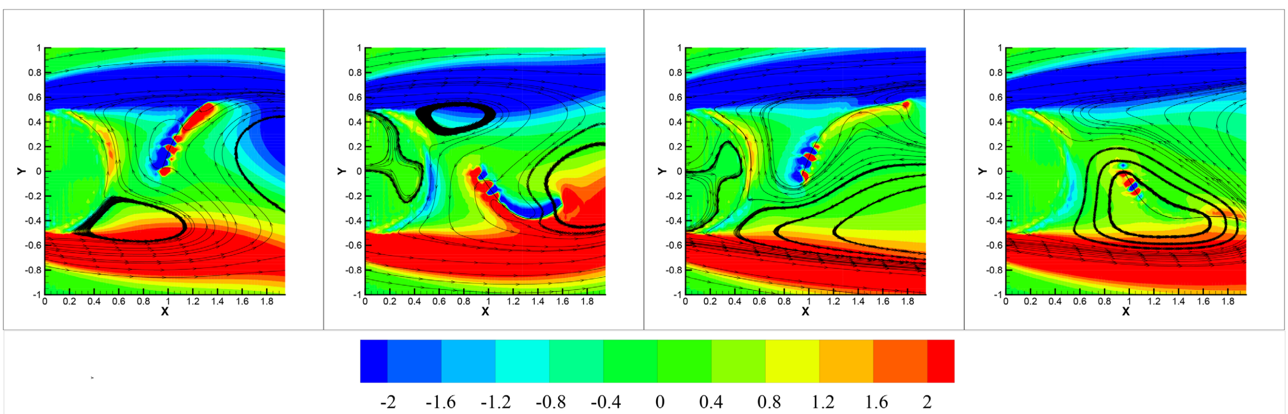

Figure 2. Flow field velocity contour.

Table 2. Velocity table of passive propulsive filament segment.

$Re = 150$	$L = 0.5$	$L = 0.75$	$L = 1.0$	$L = 1.25$
$D = 1.0$	0.048/0.118/0.300	0.076/0.166/0.260	0.064/0.116/0.220	0.068/0.086/0.192
$D = 1.5$	---	0.050/0.062/0.064	0.070/0.086/0.166	---
$D = 2.0$	---	---	0.106/0.116/0.106	---

Table 3. Average propulsive velocity of passive propelled filaments.

$Re = 150$	$L = 0.5$	$L = 0.75$	$L = 1.0$	$L = 1.25$	$L = 1.5$
$D = 1.0$	0.155	0.167	0.133	0.115	---
$D = 1.5$	---	0.058	0.107	---	---
$D = 2.0$	---	---	0.109	---	---

after the filaments release to full freedom. when $D = 1.0$, the filament's passive propulsion velocity increases first and then decrease with the increase of length. Under this condition, the filament's passive propulsion velocity reaches its maximum when $L = 0.75$. When $D = 1.5$, the maximum advance velocity of the filament appears at $L = 1.0$. When $L = 0.75$, the propulsive velocity of the filament decreases by 65.26% with the increase of the distance between the end of the filament and the center of the cylinder. When $L = 1.0$, the propulsive velocity of the filament decreases with the increase of the distance between the head end and the center of the cylinder, but the velocity change is not as obvious as that of the shorter filament.

The results show the propulsion velocity increases gradually after the release of the filament in the process of passive propulsion. The change of length and position will affect the propulsive velocity of the filament. When the positions of different lengths of filaments change, the average propulsive velocity changes with the same rule but different amplitude.

3.2. Analysis of the Force of Filament

The reason for this difference is that the force of filaments under different working conditions is different. Figure 3(a) shows the change of drag of the filament with time within 1.5 s under $D = 1.0$; $L = 0.5/0.75/1.0/1.25$. The forces of the four lengths of filaments fluctuate approximately symmetrically around 0, and the amplitude of the fluctuations increases gradually with the increase of time. However, there are still differences: From 0 to 0.5 s, the force of filament $L = 0.75$ is maximum, followed by $L = 1.0/1.25$, and $L = 0.5$ is minimum. From 0.5 - 1.0 s, the force of filament $L = 0.75$ is maximum, followed by $L = 0.5/L = 1.0$, and $L = 1.25$ is minimum. At 1.0 - 1.5 s, the force of filament $L = 0.5$ is maximum, followed by $L = 0.75/1.0$, and $L = 1.25$ is minimum. The drag results are consistent with the average velocities of different lengths of filaments in different time periods, as shown in Table 3. $D = 1.5$; $L = 0.75/1.0$ also conform to the above rules.

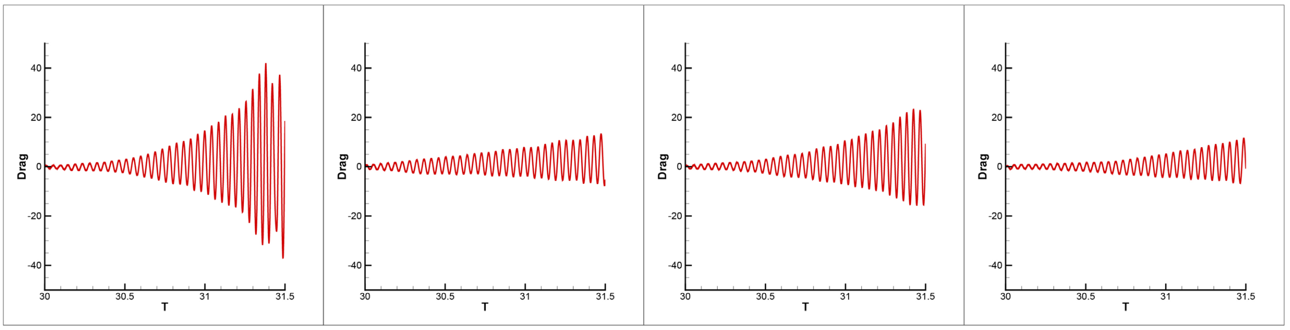

(a)

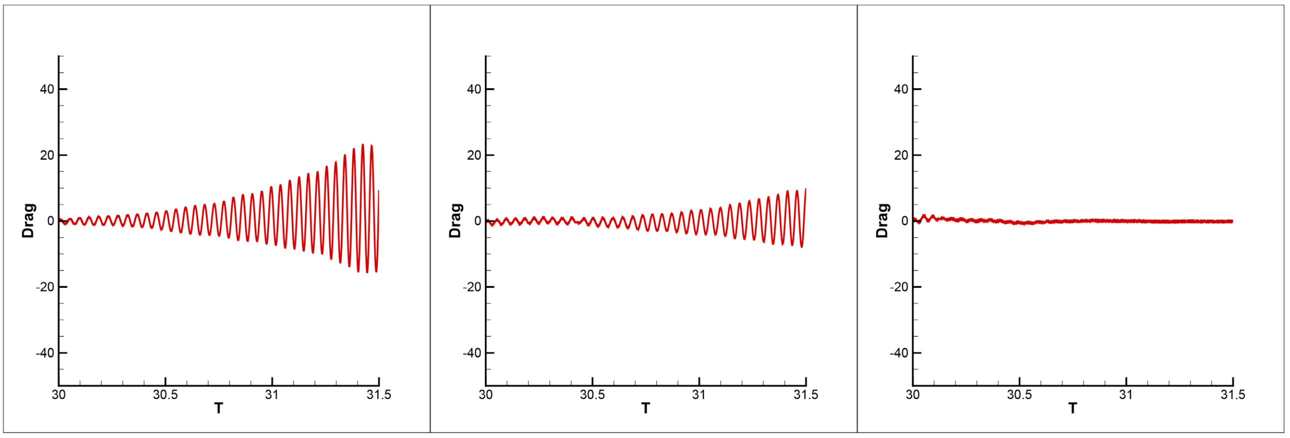

(b)

Figure 3. Drag of filaments under different working conditions.

Figure 3(b) shows the change of drag of the filament with time within 1.5 s under the working condition of $L = 1.0$; $D = 1.0/1.5/2.0$. With the increase of the distance between the head of the filament and the center of the cylinder, the drag of the filament decreases gradually, and so does the velocity of the filament. That is, the filament is further away from the cylinder, the slower the propulsion velocity, as shown in Table 3. The conditions $L = 0.75$ and $D = 1.0/1.5$ also conform to the above rules.

The distribution of pressure field around the filaments is varied with the change of length and position, which determines the force acts on the filaments, and the force further affects the propulsion velocity. The difference of the force of the filament under every working condition is caused by the different distribution of the pressure field around the filament. Figure 4 working conditions the same as Figure 2, analysis of flow field around filaments: the pressure at the end of the filament is greater than the pressure at the head. The existing pressure gradient causes the filament to receive forward force, so there is forward velocity around the filament. In addition, the farther away from the cylinder, it will get the lower the pressure gradient, and will get the smaller force acts on the filaments, then the propulsion velocity is slow. The length influence on the pressure of the surrounding flow field is the same as that of distance, that is, the flow field pressure around the filaments farther away from the center of the cylinder is smaller. It is

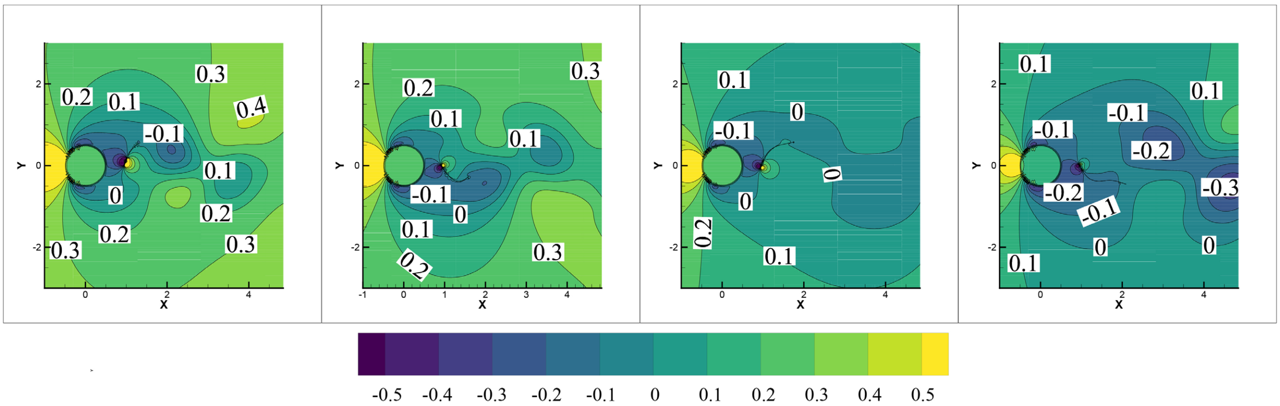

Figure 4. Pressure contour map of flow field around filaments.

precisely because of the different distribution of pressure field around the filaments that the forces of the filaments are different, so the advancing speed of the filaments under every working condition is different.

3.3. Filament Propulsive at Balance Position

In addition, in the process of exploring the effect of position change on the propulsion of the filament, it is found that there is an equilibrium position of the filament in the flow field. As the further increase of the distance between the tip of the filament and the center of the cylinder, When $L = 1.0$, $D = 2.5$, the filament cannot complete self-propelled motion.

Further calculation of $L = 1.0$, $D = 2.0\sim2.5$ shows that: there is an equilibrium position at $D = 2.475$ where the filaments neither advance nor fall with the flow. The propulsive velocity of the filaments in equilibrium mode is 0, and its propulsive posture is different from the above 7 groups of filaments, as shown in Figure 5.

As shown in Figure 6, analysis of balance position of filaments in passive propulsion can find that the flow field around the filament at the equilibrium position is symmetrical distribution along the center of the filament, the pressure field around the filament is simple distribution, there is no pressure gradient at both ends of the filament head and tail, the force on the filament is 0, and the propulsive velocity of the filament is 0. The experimental results also provide the experimental basis for swimming fish can stay be-hind the blunt cylinder.

4. Conclusions

In this paper, the immersion boundary method and the full freedom elastic filament model are used to simulate the passive propulsion of a single fish after the cylindrical wake.

1) The change of length and position will affect the velocity of filament self-propelled motion. The length and position will change the pressure difference around the filament, and the change of the filament force will lead to the change of the self-propelled velocity. In addition, the further away the filament is

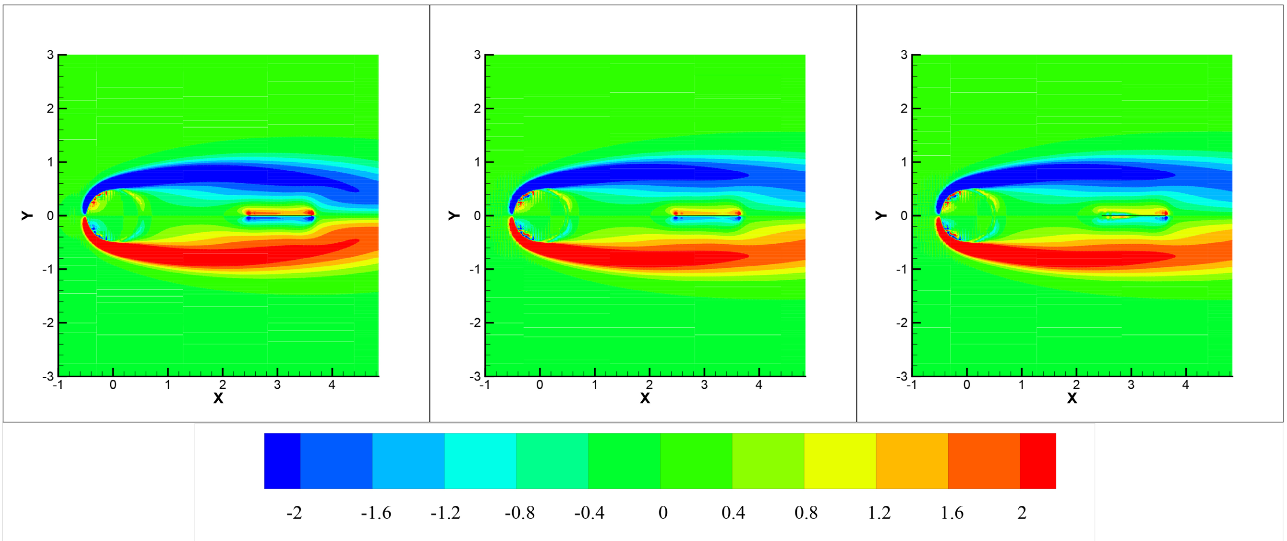

Figure 5. Contour of filament motion at equilibrium position.

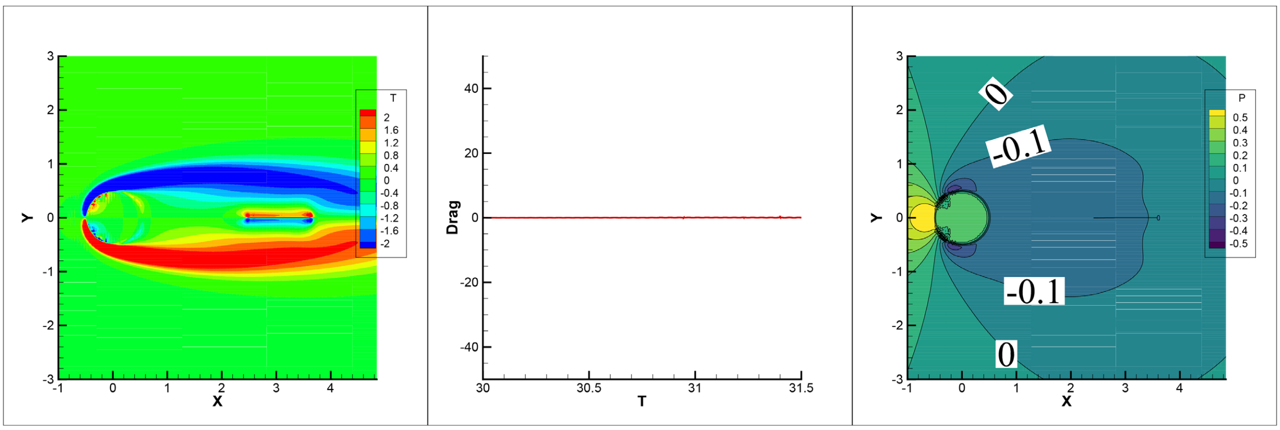

Figure 6. Contour, drag and flow field of the filament at the equilibrium position.

from the cylinder, the smaller the force, the slower the propulsion velocity, until the equilibrium position is reached, the propulsion velocity is 0.

2) There is a balance position between the passive advance of filaments and the flow down motion of filaments, under this condition, the force of the filament is 0, and the propulsive velocity is 0. The filaments neither advance nor follow the flow.

Through the above experiments, it is verified that the filaments can obtain energy from the surrounding flow field to maintain self-propelled motion, and it also provides a theoretical basis for the motion of swimming fish behind the blunt body, and the law of the pressure field and propulsion velocity with the length and position is obtained. It provides a reference for further revealing the fish swimming mechanics, and helps to develop a low resistance energy harvesting device of fish-like swimming.

Acknowledgements

This work is supported by the National Natural Science Foundation of China (grant number 12362026 and 11862017).

Conflicts of Interest

The authors declare no conflicts of interest regarding the publication of this paper.

References

[1] Dai, L., He, G. and Zhang, X. (2016) Self-Propelled Swimming of a Flexible Plunging Foil near a Solid Wall. *Bioinspiration & Biomimetics*, **11**, 046005. https://doi.org/10.1088/1748-3190/11/4/046005

[2] Wang, S., He, G. and Zhang, X. (2016) Self-Propulsion of Flapping Bodies in Viscous Fluids: Recent Advances and Perspectives. *Acta MechanicaSinica*, **32**, 980-990. https://doi.org/10.1007/s10409-016-0578-y

[3] Zhu, X., He, G. and Zhang, X. (2014) How Flexibility Affects the Wake Symmetry Properties of a Self-Propelled Plunging Foil. *Journal of Fluid Mechanics*, **751**, 164-183. https://doi.org/10.1017/jfm.2014.310

[4] Pappalardo, F. and DeRosis, A. (2014) Fluid Forces Enhance the Performance of an Aspirant Leader in Self-Organized Living Groups. *PLoS ONE*, **9**, e114687. https://doi.org/10.1371/journal.pone.0114687

[5] Becker, A.D., Masoud, H., Newbolt, J.W., *et al.* (2015) Hydrodynamic Schooling of Flapping Swimmers. *Nature Communications*, **6**, 8514. https://doi.org/10.1038/ncomms9514

[6] Wu, C.J. (2011) Energy Saving Mechanism of "Channeling Effect" in Fish School Swimming. *Chinese Journal of Theoretical and Applied Mechanics*, **43**, 18-23.

[7] Hemelrijk, C.K., Reid, D.A.P., Hildenbrandt, H., *et al.* (2015) The Increased Efficiency of Fish Swimming in a School. *Fish and Fisheries*, **16**, 511-521. https://doi.org/10.1111/faf.12072

[8] Zhu, X., He, G. and Zhang, X. (2014) Flow-Mediated Interactions between Two Self-Propelled Flapping Filaments in Tandem Configuration. *Physical Review Letters*, **113**, 238105. https://doi.org/10.1103/PhysRevLett.113.238105

[9] Jian, D., Xuerui, M. and Luca, B. (2021) Symmetry Breaking of Tail-Clamped Filaments in Stokes Flow. *Physical Review Letters*, **126**, 124501. https://doi.org/10.1103/PhysRevLett.126.124501

[10] Liu, L., He, G.Y., He, X.Y. and Wang, Q. (2022) Effect of Flexibility on the Motion State of Filament in Vortex Streets. **13**, 51-59.

[11] Lin, X.J., He, G.Y., He, X.Y. and Wang, Q. (2018) Dynamic Response of a Semi-Free Flexible Filament in the Wake of a Flapping Foil. *Journal of Fluids and Structures*, **83**, 40-53. https://doi.org/10.1016/j.jfluidstructs.2018.08.009

[12] Peskin, C.S. (1972) Flow Patterns around Heart Valves: A Numerical Method. *Journal of Fluids and Structures*, **10**, 252-271. https://doi.org/10.1016/0021-9991(72)90065-4

[13] Lin, X., He, G., He, X., Wang, Q. and Chen, L. (2017) Numerical Study of the Hydrodynamic Performance of Two Wiggling Hydrofoils in Diagonal Arrangement. *Journal of Applied Mathematics and Physics*, **3**, 31-38. https://doi.org/10.4236/jamp.2017.51005